HIGH SPEED JET CONTROL USING PLASMA ACTUATORS

M. Samimy[1], J.-H. Kim[1], I. Adamovich[2], Y. Utkin[2], and S. Keshav[2]
Department of Mechanical Engineering, The Ohio State University
Columbus, Ohio 43235-7531USA
samimy.1@osu.edu

ABSTRACT

We have made significant progress in our on-going research in the development of localized arc filament plasma actuators and their application to control high-speed and high Reynolds number flows. We used a newly developed plasma generator to drive eight actuators distributed around the perimeter of a 2.54 mm diameter axisymmetric nozzle just upstream of the exit. The flow exiting the nozzle was an ideally expanded Mach 1.3 jet with a Reynolds number of over a million. The plasma generator could drive all eight actuators with any prescribed frequencies from 0 to 200 kHz, phase, and duty cycle. Only control frequencies over the range of 2 kHz to 20 kHz (St_D of 0.13 to 1.3) were explored for this paper. While jet responded to control over the entire range of frequencies covered, robust and highly spatially coherent structures were generated over the range of St_D of 0.33 to 0.6. Tremendous jet mixing enhancement was achieved with the use of first helical mode forcing over the range of St_D of 0.2 to 0.4. The power consumption for all eight actuators was less than 1% of the flow power.

INTRODUCTION

Passive control of jets and mixing layers via geometrical modifications of nozzle/splitter plate trailing edge (e.g. using tabs, chevrons, lobbed nozzles) has been extensively used (e.g. Samimy et al. 1993, Zaman et al. 1994, McCormick and Bennett 1994, Kim and Samimy 1999, Saiyed et al. 2003). For active control, one or more of the jet instabilities must be manipulated. There are several instabilities associated with a jet, which have been well researched in low-speed and low Reynolds number jets (e.g. Crow and Champagne 1971, Kibens 1979, Zaman and Hussain 1981, Ho and Huerre 1984, and Cohen and Wygnanski 1987). The first one is the jet initial shear layer instability, which is also called Kelvin-Helmholtz instability or inviscid instability. The frequency of this instability scales with the momentum thickness (θ) of the boundary layer at the nozzle exit. The maximum amplification of disturbances seems to occur around the Strouhal number ($St_\theta=f\theta/U_j$) of 0.012 (e.g. Zaman and Hussain 1981), while the maximum amplification rate of disturbances occur around $St_\theta=0.017$ (Michalke 1965). The input excitation amplitude required to control this instability in low speed flows is very small and linear instability analysis has been used extensively to explore various aspects of this instability (e.g. Michalke 1965). The growth of this instability leads to the large scale structures in the shear layer of the jet, which are responsible for the entrainment of ambient air into the jet and gross mixing with the jet fluid.

The second jet instability is called jet column or jet preferred mode instability, which scales with the nozzle exit diameter for a round jet or nozzle exit height for a rectangular jet ($St_D=fD/U_j$). The maximum amplification of this instability occurs over a wide range of St_D from 0.2 to 0.6 (Crow and Champagne 1971 and Gutmark and Ho 1983), heavily depending upon the experimental facility. This is presumably due to the variations of the naturally occurring disturbances in the experiments. In addition, one would expect a dependency on how close the jet column instability frequency is to one of the sub-harmonics of the initial shear layer instability frequency in a given experiment. As the shear layers of the jet grow and merge and the thickness of the combined shear layer approaches the diameter or height of the nozzle, azimuthal instabilities (flapping mode for the rectangular jet and helical and flapping modes for the axisymmetric jet) begin to amplify (Cohen and Wygnanski 1987). Further, one could combine two instability modes (e.g. axisymmetric and azimuthal) to achieve greater control such as jet bifurcation or blooming (Parekh et al. 1996; Reynolds et al. 2003).

Many researchers over several decades have contributed to the control of low-speed and low Reynolds number jets and the understanding of the physics and mechanisms of jet response to such control. The upper edge of the Reynolds number based on jet diameter seems to be around 50,000 for these works. As the speed and the Reynolds number of the jet increase, so do the background noise, the instability frequencies, and the flow momentum. Therefore, actuators must provide excitation signals of much higher amplitude and frequencies - two diametrically opposing requirements. As a result, there is practically no work in the active control of high-speed and high Reynolds number jets, with a couple of exceptions. Kibens et al. (1999) used high amplitude pulsed injection to excite the exhaust from a full-scale jet engine at a flapping mode (they used two actuators 180° out of phase, and each covering a 1/4 of the perimeter of the jet), which resulted in significantly increased mixing and noise radiation. Obviously, the increased scale and thus the reduced frequency was a key factor in this work. Also, Ahuja et al. (1982) and Lepicovsky et al. (1987) used acoustic forcing, but channeled the acoustic signal to multiple locations at the proximity of the exit of the jet, rather than using typical global type forcing, to force a high subsonic jet around its preferred mode.

We have recently developed a class of plasma actuators, called localized arc filament plasma actuators (LAFPA) that can provide excitation signals of high amplitude and high frequency for high-speed and high Reynolds number flow control (Samimy et al. 2004 a & b). In the following sections, we will first provide a brief overview of the experimental set up and techniques followed by a description of these actuators. We will then present some exciting results in controlling a supersonic jet using these actuators.

---

[1] Gas Dynamics and Turbulence Laboratory
[2] Nonequilibrium Thermodynamics Laboratory

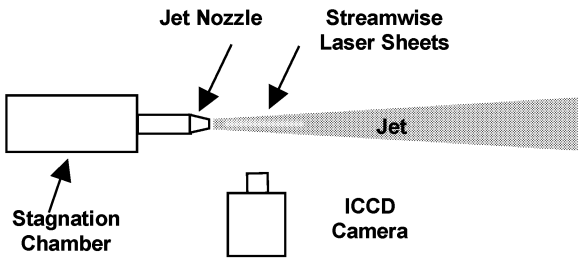

Figure 1: Schematic of the jet facility and the planar flow visualization set up.

EXPERIMENTAL FACILITY AND TECHNIQUES

The Flow Facility

All the experiments were conducted in the Gas Dynamics and Turbulence Laboratory at The Ohio State University. The ambient air is compressed, dried, and stored in two cylindrical tanks at a pressure of up to 16 MPa with a capacity of 36 m^3. The compressed air is supplied to the stagnation chamber and conditioned before entering into a Mach number 1.3 axisymmetric converging-diverging nozzle, which is designed using the Method of Characteristics for uniform flow at the nozzle exit. The air is discharged horizontally through the nozzle into an anechoic chamber (Fig. 1). The nozzle has an exit diameter of 2.54 cm (1.0"). A nozzle extension, made of boron nitride, was attached to the exit of the nozzle to house the plasma actuators.

The actual Mach number of the jet was measured to be 1.35. The Reynolds number of the jet based on the jet diameter was about 1.0×10^6. The boundary layer thickness at the exit of the nozzle is very thin, which makes it impossible to obtain a boundary layer profile to estimate its momentum thickness and its state. Kastner et al. (2004) attached a converging nozzle of similar length to this facility and measured a few points within the boundary layer of a Mach 0.9 jet. They estimated the boundary layer to be turbulent with a thickness of about 1 mm and a momentum thickness of about 0.1 mm. The characteristics of the boundary layer in the current experiments should be quite similar.

THE FLOW DIAGNOSTIC TECHNIQUES

The flow was visualized using scattering of light from a laser sheet passing through the centerline of the jet (Fig. 1). The particles scattering light were formed in the mixing layer of the jet when the moist but warm ambient air was entrained into the jet and mixed with the cold but dry jet air. Either Spectra Physics Quanta-Ray Pro or PIV-400 Nd:YAG laser was used as a light source. The scattered laser light was captured by a Princeton Instrument ICCD camera, located normal to the laser sheet (Fig. 1). Thus instantaneous planar images of the jet with 9 ns exposure time (the laser pulse duration) were acquired. In this visualization technique, a major portion of the mixing layer was visualized since no condensation occurs in the jet core or the ambient air.

The streamwise images of the jet were taken either randomly or phase-locked to the input signal to the transistor switch of an actuator. A 10 Hz TTL signal generated by a pulse counter, phase-locked to the input signal, was directed to the laser Lamp-Trigger input and the laser Lamp-Sync output was used to trigger the camera. A custom-built circuit was used to isolate laser and imaging systems from the TTL signal to the transistor switches.

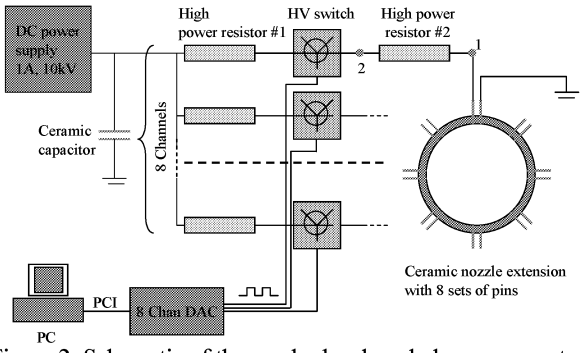

Figure 2: Schematic of the newly developed plasma generator.

The centerline stagnation pressure was measured by a 1.5 mm outer diameter pitot tube, which was moved along the jet centerline with a manual traversing system. From the stagnation pressure, the centerline Mach number was calculated by assuming that the local static pressure was the same as the ambient pressure. This was a reasonable assumption, as the jet was operating in the ideally expanded flow regime. A planar imaging velocimetry system is currently being used for detailed velocity measurements. These results will be presented in a later publication.

PLASMA ACTUATORS AND PLASMA GENERATOR SYSTEM

Each actuator consists of a pair of pin electrodes. The electrodes are distributed around the nozzle perimeter (Fig. 2), approximately 1 mm upstream of the nozzle exit plane. A ring groove of 0.5 mm deep and 1 mm wide located to house the electrodes and to shield and stabilize the plasma. In our earlier experiments, the plasma was blown away without such a groove. We have used various nozzle extensions attached to the nozzle exit to house the electrodes, as well as various kind and size electrodes (Samimy et al. 2004 a & b). For the work presented here, the nozzle extension was made of boron nitride and steel piano wires of 1 mm diameter were used for electrodes. Measured center-to-center, the spacing between a pair of electrodes for each actuator is 3 mm, and the distance between the neighboring electrodes of two adjacent actuators is 6 mm. With this arrangement, the actuators were not uniformly distributed around the nozzle extension, as shown in Figure 2, but there was a little more distance between the top four and bottom four actuators. This was taken into account in forcing the jet in helical mode.

In the previous work, we used an AC power supply that consisted of two 1500 W amplifiers connected to a two-arm step-up high voltage transformer (Samimy et al. 2004 a & b). The 1-10 V peak-to-peak sinusoidal wave input to the amplifiers was supplied by a function generator. A 500 Ohm ballast resistor was connected in series on the ground side of every actuator. The dual channel power supply could power up to two actuators with variable phase shift between the actuators. With two AC power supplies used, up to four actuators could be powered, depending on the frequency range of interest within 2 to 100 kHz.

Figure 2 shows a schematic of the new multi-channel high-voltage plasma generator, designed and built in-house at

The Ohio State University. The plasma generator enables simultaneous powering of up to eight arc filament plasma actuators distributed around the perimeter of the ceramic nozzle extension, with independent frequency, duty cycle, and phase control of individual actuators. Each actuator is connected in series with a fast response, high repetition rate, high-voltage transistor switch, two approximately 15 kΩ high power solid body ceramic ballast resistors, and a high-voltage, high-current (10 kV, 1A) Glassman DC power supply (Fig. 2). Two of these power supplies are used to energize eight actuators. If all eight actuators are powered at the same time, the single actuator current is limited to 0.25A. The switches are controlled by using an 8-channel digital-to-analog output PCI card and the LabView software, which allows their independent frequency, duty cycle, and phase control. The switches are capable of producing high voltage pulses (up to 8 kV) at repetition rates from 0 to 200 kHz, with a very short pulse rise/fall time (~0.1 μsec) and a variable duty cycle (from 0 to 100%). Every switch is liquid cooled to allow continuous operation at high frequencies, voltages and high currents.

By turning the electronic switch on and off, positive high voltage pulses can be applied to the corresponding actuator. The high initial voltage is needed to produce breakdown in the atmospheric pressure air in the gap between the two electrodes of an actuator, which are 3 mm apart in the present work. After the breakdown, the arc is generated and the voltage across the gap rapidly falls to a few hundred volts. The plasma generator is compact, robust, and simple to operate. A continuous operation of all eight actuators in the Mach 1.3 flow of the current work (up to several minutes) has been achieved. A significant reduction in electromagnetic wave radiation was achieved by implementing a house-built circuit on the lower voltage side of the input signal.

EXPERIMENTAL RESULTS

This is an on-going research and in its initial stages. We reported the concept and initial characterization of local arc filament plasma actuators using commercially available AC power supply in Samimy et al. (2004b) and some initial results on the application of the actuators for jet control in Samimy et al. (2004a). Since then, as we discussed earlier, we have developed a new and much more capable plasma generator based on DC power supply and transistor switches. The new plasma generator can drive up to 8 actuators with frequencies from 0 to 200 kHz, and any prescribed duty cycle and phase. Below we will first present some results on the characteristics of the plasma actuators using the new plasma generator. We will then present some interesting results on the use of these actuators to control the flow in the ideally expanded Mach 1.3 axisymmetric jet with a Reynolds number of about 1 million.

PLASMA ACTUATOR CHARACTERIZATION

Figure 3 shows time-dependent voltage, current, and power in the arc discharge between two pin electrodes of a plasma actuator. During these measurements, eight actuators were operated in a helical mode at 5 kHz frequency and a 20% duty cycle in the ideally expanded Mach 1.3 jet. The static pressure at the actuators location (1 mm before the nozzle extension exit) was 1 atm. The top graph shows time-dependent voltage between the actuator electrodes, measured at point 1 (Fig. 2) by a Tektronix high voltage probe P6015A. A very large voltage overshoot (about 7.4 kV, not fully

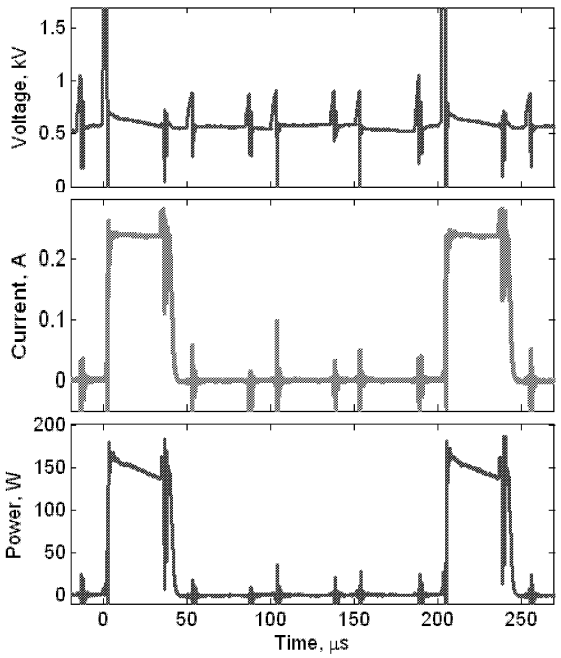

Figure 3: Time-dependent voltage, current, and power in a plasma actuator operated at 5 kHz frequency and 20% duty cycle (all eight actuators are powered in a helical mode).

resolved in this figure) at the onset of the cycle (t = ~60 μs on the graph) corresponds to electrical breakdown in the air between the electrodes, followed by a sharp voltage drop to about 500 V, as a stationary arc discharge is formed. After the discharge current is interrupted by rapidly closing the switch (40 μs later), the plasma is quickly blown off by the flow. Because of this, the high voltage electrode (anode) becomes floating and the voltage remains essentially unchanged (at about 500 V) until the moment the switch is opened again 200 μs later (Fig. 3). Smaller voltage spikes between the two larger ones are due to EMI interference generated when other actuators are turned on and off.

The actuator current measured at the same time using a Tektronix AM503S current probe is shown in the middle graph in Fig. 3. It can be seen that the current trace is nearly a step function, with the steady state current of about 0.25A when the switch is open and no current when it is closed. The time-dependent arc discharge power can be obtained simply by multiplying the current and the voltage traces. The result is shown in the bottom graph in Fig. 3. One can see that the power during the current pulse reaches approximately 150W, which corresponds to the time-averaged actuator power of only 30 W (i.e. 240W net power for all eight actuators in operation). For comparison, the flow power (the total enthalpy flux) at these conditions is about 28 kW. This result demonstrates that high-speed flow control by localized arc plasma actuators can be highly energy efficient.

The measurements showed that the voltage, current, and power traces for all eight actuators are essentially the same except for a phase shift. Depending on the frequency, phase shift, and duty cycle the arc discharges produced by different actuators may overlap in time. Interference caused by other actuators in the form of very short voltage and current spikes corresponding to the moments of time when these actuators

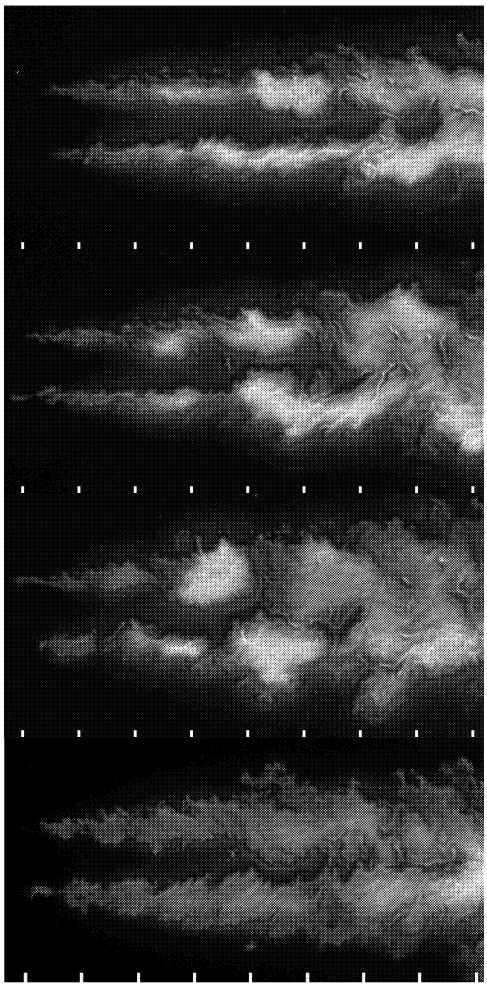

Figure 4: Instantaneous streamwise planar images of the baseline jet and jet at first helical mode forcing frequency of 3, 5, and 12 kHz. The spacing between adjacent tick marks is one nozzle diameter and the first tick mark is at x/D = 1.

are switched on and off can be seen in Fig. 3. However, this interference has no apparent effect on discharge power (Joule heating) coupled to the flow and therefore should not affect the flow control. With only one actuator running (the results not shown here), the EMI interference spikes disappear, while the actuator current remains very nearly the same.

Running the actuators at a higher frequency of 20 kHz and a lower duty cycle of 10%, it was noticed that the actual duty cycle was somewhat smaller (only about 5%) due to a delay between the onset of the voltage and the current pulses. Indeed, it was seen that it took about 5 μsec for the current pulse to rise after the switch opens and high voltage is applied to the actuator electrodes.

FLOW RESULTS

In this section, some initial flow visualization results using planar laser sheet illumination will be presented. Both instantaneous and phase-averaged (ensemble averaged in the unforced case) planar images will be presented. While these images could be used for qualitative assessment of the control of the jet using plasma actuators, spatial correlation of the

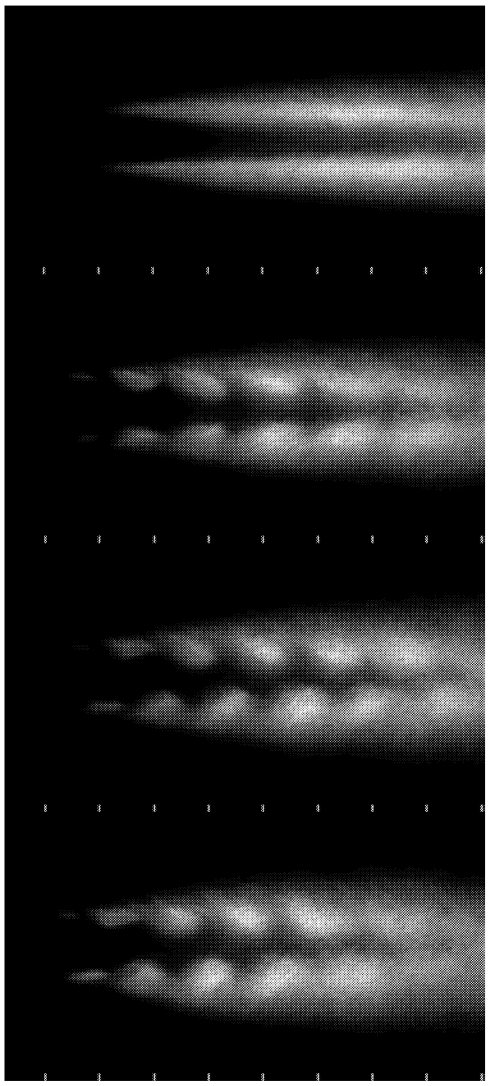

Figure 5: Images from top to bottom: ensemble averaged baseline jet and phase averaged jet at 9 kHz forcing with axisymmetric, flapping, and first helical modes.

images as well as the jet centerline Mach number profiles, obtained using a pitot tube, will be presented for quantitative assessment of the control.

The newly constructed plasma generator could power up to eight actuators from 0 to 200 kHz. However, the initial results will focus on a range of frequencies that covers only the jet column instability. The major parameters that are expected to influence the jet control are the forcing frequency, duty cycle of the input signal, mode of actuation (e.g. axisymmetric, helical), the input voltage, and the electrode spacing. For the results presented here, the electrode spacing was fixed at 3 mm and the effect of input voltage was not investigated. However, over the frequency range of 2 kHz (St_D = 0.13) to 20 kHz (St_D = 1.3), we have investigated the effects of duty cycle and some limited modes (axisymmetric, flapping, and 1st helical) in controlling the jet. Figure 4 shows instantaneous planar images of the flow for the baseline case and the first helical forcing at three frequencies at 3, 5, and 12

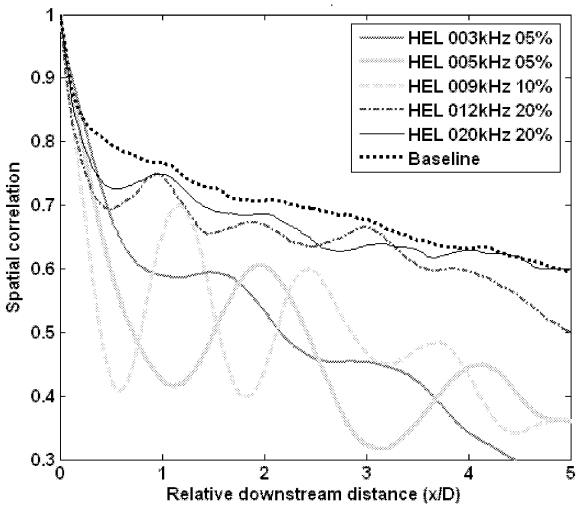

Figure 6: Averaged spatial correlation of images along the approximate centerline of the jet shear layer (taken from two-dimensional spatial correlation) for the baseline jet and forced jet with the first helical mode at various frequencies.

kHz). The duty cycle was varied to achieve the optimal forcing for the given forcing frequency. While the forcing is effective over the entire frequency range of St_D = 0.13 to 1.3, it is optimum in generating the most robust large scale structures for St_D ~0.33. This is consistent with the results in the literature for the most amplified jet column range of 0.2 to 0.6 (e.g. Kibens 1980 and Cho et al. 1998).

Figure 5 shows ensemble average of 35 instantaneous images of the baseline jet (similar to the one shown in Fig. 4) and 35 phase-averaged images for three different actuation modes at 9 kHz. The coherent structures are distinct and robust in all three forcing modes, but the first helical mode seems to have the strongest impact.

A statistical analysis of the instantaneous images of the jet, such as those shown in Fig. 4, was used to investigate the periodic nature of structures in the baseline and controlled jet and thus more objectively assess the effect of control. A small template or window, which covers the entire width of the top or bottom shear layer and whose length was slightly larger than the forcing wavelength in the streamwise direction, was manually or semi-manually selected, and the two-dimensional spatial correlation between the image within the template and the rest of the images (of either top or bottom shear layer) was calculated. Details of the procedure can be found in Thurow et al. (2003). The two-dimensional spatial correlation is then averaged over 50 instantaneous image cases. Figure 6 shows the spatial correlation along a horizontal line passing through the peak of the two-dimensional correlation for helical mode actuations. Note that the floor level (the level about which the peaks and valleys fluctuate) for each curve depends on the selection of the template and background intensity level. Thus, one should focus on the difference between the amplitude of (correlation level of) peaks and valleys for each correlation curve. A sinusoidal profile with large amplitude indicates that robust periodic structures were generated by the forcing. Unlike the baseline case, periodic structures are seen in Figure 6 for all the helical forcing cases from 3 to 20 kHz. The periodicity of these structures is quite robust, as indicated by the strong correlation peaks and valleys, in the mid-frequency

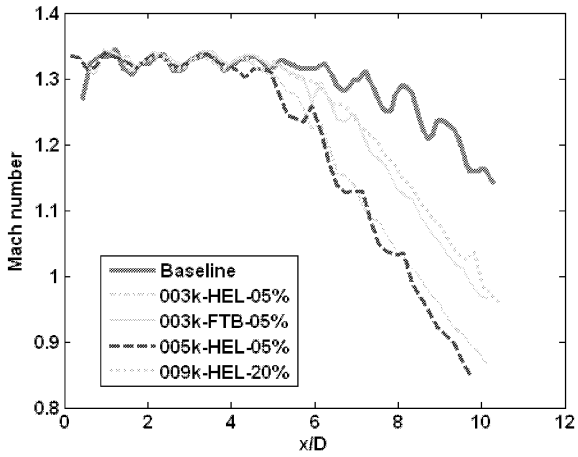

Figure 7: Mach number of the jet along the jet centerline for the baseline case and three forced cases with first helical mode of various frequencies and one forced case with flapping mode at 3 kHz.

range of 5-9 (St = 0.33-0.6). However, the periodicity gradually decays away from this range on either side of it.

Any major changes in the characteristics of large-scale structures in the mixing layer of the jet, which are responsible for the entrainment of the ambient air into the jet and gross mixing, are reflected in the centerline properties such as Mach number or velocity. Figure 7 shows the average centerline Mach number of the jet, measured by a pitot tube, for the baseline jet and for four forced cases. All four forced cases show shortened jet core, indicating more mixing. For example, the jet core length is about 5.5D for the 5 kHz forcing case, in comparison to 7.0D for the baseline case. Also, the decay rate of the centerline Mach number beyond the jet core is significantly higher for the helical mode forcing at 3 and 5 kHz, which is higher than that for the 3 kHz flapping mode or 9 kHz helical mode forcing, which in turn is much higher than that of the baseline case. These quantitative results confirm the qualitative results shown earlier and show dramatic effects of forcing on this Mach 1.3 high Reynolds number jet. The results also confirm that the helical forcing around St_D of about 0.33 generates the most robust large-scale structures as well as the most enhanced mixing.

CONCLUDING REMARKS

We presented and discussed significant progress that we have made in our on-going research endeavor in the development of localized arc filament plasma actuators and their application to control high-speed and high Reynolds number flows. In our earlier work we had reported results on the concept of these actuators (Samimy et al. 2004b) and very preliminary results on jet control (Samimy et al. 2004a). These actuators work by way of pulsating local heating of the flow and as a result the actuators must be distributed in the flow in order to feed the flow with disturbances of desired frequencies to force flow instabilities. One major concern was the lack of any commercially available power supply capable of driving multiple of these actuators over a range of frequencies. We have recently developed a DC power supply and high voltage transistor switch based plasma generator capable of driving eight actuators with any prescribed frequencies from 0 to 200

kHz, phase, and duty cycle. We used this plasma generator to drive eight actuators distributed around the perimeter of a 2.54 mm diameter axisymmetric nozzle, approximately 1 mm upstream of the jet exit. The flow exiting the nozzle was an ideally expanded Mach 1.3 jet with a Reynolds number of over a million. Only control frequencies over the range of 2 kHz to 20 kHz (St_D of 0.13 to 1.3) were explored for this paper.

Various flow diagnostic techniques were used to assess the effects of forcing. The jet responded to the control signal with varying degrees over the entire range of frequencies covered, the forcing mode, and also the duty cycle of the forcing input signal. Most robust and highly spatially coherent structures were generated only over the range of St_D of 0.33 to 0.6, with the duty cycle of less than 30%, and with either the flapping or first helical mode. A tremendous jet mixing enhancement was achieved over the range of St_D of 0.2 to 0.4 with the first helical mode forcing. The power consumption for the all 8 actuators was less than 1% of the flow power. These actuators impose significant authority over the jet over a wide range of variables space. The presented results show only the potential of this control technique and lots more remain to be explored.

ACKNOWLEDGEMENTS

The partial support of this research by NASA Glenn Research Center and by the Ohio Center for Advanced Propulsion and Power (OCAPP) is greatly appreciated.

REFERENCES

Ahuja, K.K., Lepicovsky, J., Burrin, R.H., 1982, "Noise and Flow Structure of a Tone-Excited Jet," AIAA J., Vol. 20, No. 12, 1700-1706.

Cho, S.K., Yoo, J.Y., and Choi, H., 1998, "Vortex pairing in an axisymmetric jet using two-frequency acoustic forcing at low to moderate Strouhal numbers," Experiments in Fluids, Vol. 25, 305-315.

Cohen J. and Wygnanski I., 1987, "The evolution of instabilities in the axisymmetric jet. Part 1. The linear growth of disturbances near the nozzle," *Journal of Fluid Mechanics*, Vol.176, 191-219.

Crow, S.C. and Champagne, F.H., 1971, "Orderly Structure in Jet Turbulences," Journal of Fluid Mechanics, Vol. 48, 547-591.

Gutmark, E. and Ho, C.M., 1983, "Preferred Modes and the Spreading Rated of Jets," Phys. Fluids, Vol. 26, No. 10, 2932-2938.

Ho, C-M, and Huerre, P., "Perturbed Free Shear Layers," *Ann. Rev. Fluid Mech.*, Vol. 16, pp. 365-424, 1984.

Kastner, J., Hileman, J., and Samimy, M., 2004, "Exploring High-Speed Axisymmetric Jet Noise Control Using Hartmann Tube Fluidic Actuators," AIAA Paper 2004-0186.

Kibens, V., 1980, "Interaction of Jet Flowfield Instabilities with Flow System Resonance," AIAA Paper 1980-0963.

Kibens, V., Dorris. J., Smith, D.M., and Mossman, M.F., 1999, "Active Flow Control Technology Transition: The Boeing ACE Program," AIAA Paper 1999-3507.

Kim, J.-H. and Samimy, M., 1999, "Mixing enhancement via nozzle trailing edge modifications in a high speed rectangular jet," Phys. Fluids, Vol. 11, No. 9, 2731-2742.

Lepicovsky, R., Ahuja, K.K., Brown, W.H., and Burrin, R.H., 1987, "Coherent large scale structures in high Reynolds number Supersonic jets," AIAA J., Vol. 25, No. 11, 1419-1425.

McCormick, D. C. and Bennett, J. C. Jr., 1994, "Vortical and Turbulent Structure of a Lobed Mixer Free-Shear Layer," AIAA J., Vol. 32, 1852-1859.

Michalke, A., 1965, "On Spatially Growing Disturbances in an Inviscid Shear Layer," Journal of Fluid Mechanics, Vol. 23, 521-544.

Parekh, D. E., Kibens, V., Glezer, A., Wiltse, J. M., and Smith, D. M., 1996, "Innovative Jet Flow Control: Mixing Enhancement Experiments," AIAA Paper 1996-0308.

Reynolds, W.C., Parekh, D.E., Juvet, P.J.D., and Lee, M.J.D., 2003, "Bifurcating and Blooming Jets," Ann. Rev. Fluid Mech., Vol. 35, 295-315.

Saiyed, N.H., Mikkelsen, K.L. and Bridges, J.E.,2003, "Acoustics and Thrust of Quiet Separate-Flow High-Bypass-Ratio Nozzles," AIAA J., Vol. 41, No. 3, 372-378.

Samimy, M., Zaman, K.B.M.Q., and Reeder, M.F., 1993, "Effect of Tabs on the Flow and Noise Field of an Axisymmetric Jet," AIAA J., Vol. 31, No. 4, 609-619.

Samimy, M., Adamovich, I., Kim, J.-H., Webb, B., Keshav, S., and Utkin, Y., 2004a, "Active Control of High Speed Jets Using Localized Arc Filament Plasma Actuators," AIAA Paper 2004-2130.

Samimy, M., Adamovich, I., Webb, B., Kastner, J., Hileman, J., Keshav, S., and Palm, P., "Development and Characterization of Plasma Actuators for High Speed and Reynolds Number Jet Control," Experiments in Fluids, Vol. 37, No. 4, pp. 577-588, 2004b.

Thurow, B., Samimy, M., and Lempert, W., 2003, "Compressibility effects on turbulence structures of axisymmetric mixing layers," Phys. Fluids, Vol. 15, No. 6, 1755-1765.

Zaman K.B.M. and Hussain A.K.M.F., 1980, "Vortex pairing in a circular jet under controlled excitation," *Journal of Fluid Mechanics*, Vol.101, 449-491.

Zaman, K.B.M.Q. and Hussain, A.K.M.F., 1981, "Turbulence Suppression in Free Shear Flows by Controlled Excitation," J. Fluid Mechanics, Vol. 103, 133-159.

Zaman, K.B.M.Q., Reeder, M.F., and Samimy, M., 1994, "Control of an Axisymmetric Jet Using Vortex Generators," Phys. of Fluids, Vol. 6, No. 2, 778-793.